

Medical Matting: A New Perspective on Medical Segmentation with Uncertainty

Lin Wang^{1,2,3}[0000-0003-2374-0725], Lie Ju^{2,3}, Donghao Zhang², Xin Wang³, Wanji He³, Yelin Huang³, Zhiwen Yang³, Xuan Yao³, Xin Zhao³, Xiufen Ye¹, and Zongyuan Ge²

¹ Harbin Engineering University, Harbin Heilongjiang 150001, China

² Monash Medical AI Group, Monash University, Clayton VIC 3800, Australia

³ Airdoc Co., Ltd, Beijing 100089, China

{wanglin.mailbox, julie334600}@gmail.com

yexiufen@hrbeu.edu.cn

zongyuan.ge@monash.edu

Abstract. In medical image segmentation, it is difficult to mark ambiguous areas accurately with binary masks, especially when dealing with small lesions. Therefore, it is a challenge for radiologists to reach a consensus by using binary masks under the condition of multiple annotations. However, these areas may contain anatomical structures that are conducive to diagnosis. Uncertainty is introduced to study these situations. Nevertheless, the uncertainty is usually measured by the variances between predictions in a multiple trial way. It is not intuitive, and there is no exact correspondence in the image. Inspired by image matting, we introduce matting as a soft segmentation method and a new perspective to deal with and represent uncertain regions into medical scenes, namely medical matting. More specifically, because there is no available medical matting dataset, we first labeled two medical datasets with alpha matte. Secondly, the matting method applied to the natural image is not suitable for the medical scene, so we propose a new architecture to generate binary masks and alpha matte in a row. Thirdly, the uncertainty map is introduced to highlight the ambiguous regions from the binary results and improve the matting performance. Evaluated on these datasets, the proposed model outperformed state-of-the-art matting algorithms by a large margin, and alpha matte is proved to be a more efficient labeling form than a binary mask.

Keywords: Uncertainty quantification · Soft segmentation · Image Matting.

1 Introduction

Due to the limitation of imaging methods, ambiguities are common in medical images. The pathological or anatomical structures, especially those around their boundaries, can be blurred and difficult to be segmented. Hence the study of predictive uncertainty of segmentation results is as essential as improving segmentation accuracy because the trustworthiness of model output is vital for clinicians.

Generally, the uncertainty can be categorized into two types, aleatoric uncertainty and epistemic uncertainty [16,27,31]. Aleatoric uncertainty is often related to intrinsic

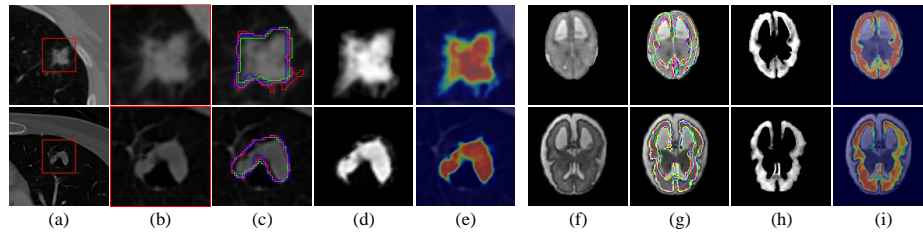


Fig. 1. Examples of the ambiguity in the medical image. (a) (b) and (f) are the original or enlarged images of lung nodule [2] and newborn brain myelination process [26]. (c) and (g) are the contours of the human binary labels. Inaccuracy and inconsistency are more likely to be located in the ambiguity regions. (d) and (h) shows the targets labeled by the alpha matte. It is more explainable than the binary labels in ambiguity regions. (e) and (i) reveals the original images mixed with the alpha matte in pseudo-color for better display. Better view in zoom and color.



Fig. 2. The most descriptive label (the alpha matte or one of the binary masks) for each medical image is evaluated by clinicians. (a) and (b) shows 100 randomly selected cases of the LIDC-IDRI and cases of the Brain-growth, respectively. Rows denote votes of clinicians, and columns denote different image cases in the two datasets. The alpha mattes (red blocks) are more preferred in expressing the anatomical structures than the binary masks (blocks in other colors).

noise in the data that hard to reduce. In contrast, epistemic uncertainty is associated with suboptimal parameters of a model due to insufficient data [9,18], which can be alleviated by providing more data. However, the difficulty in data collection and the high cost of annotation make lack of data common in medical image study, which urge us to use the insufficient data to the fullest. After observing the annotations from multiple radiologists, we found a large proportion of the discrepancies in segmentation tasks, which was thought hard to reduce, is due to the inadequate expressiveness of binary masks and the predicament of existing labeling techniques for tiny structures (see Fig. 1) and could be mitigated by a more effective labeling method.

Many research works focus on quantifying the uncertainty and alleviate its impact on segmentation for disease diagnosis and prognosis [17,18,28,20,15,3,12]. However, most of them measure the uncertainty by learning the predictions' discrepancies in various forms, such as cross-entropy or variance. It is unintuitive and hard to be evaluated visually. Besides, the binary masks may lose information for diagnosing.

Matting [1,6,8,11,21,23,25,22] is a specific segmentation approach widely used in picture editing, green screen, virtual conference, etc. It can obtain fine-grained details by introducing a blending coefficient named alpha matte α , between the foreground \mathcal{F} and background \mathcal{B} of an image \mathcal{I} , which makes $\mathcal{I} = \alpha\mathcal{F} + (1 - \alpha)\mathcal{B}$. Analogically, the uncertainty can be considered the degree of mixing the pathological tissue and its surrounding environment. However, matting methods are not widely used in medical

images and are limited as an auxiliary of segmentation [34,7,10,35]. Since uncertainty is highly coupled with the challenging regions of segmentation results and there is no clear definition of uncertainty, we introduce alpha matte into medical scenarios as calibration of uncertainty and a more accurate segmentation method.

Our contribution is summarized as follows: 1) Alpha matte is first introduced in medical scenarios, which is more expressive than binary masks by experiments. Valuable information in such regions can be reserved. 2) The uncertainty is defined more intuitively by the alpha matte. 3) A compact multi-task network was proposed, producing the alpha matte and binary masks simultaneously. 4) Uncertainty map is proposed as an analog to the trimap in image matting based on the predictions of binary masks and improves the matting network’s performance. 5) The datasets labeled for uncertainty learning and medical matting are publicly available as benchmark datasets for the research community. The code and datasets can be achieved from <https://github.com/wangsssky/MedicalMatting>.

2 Datasets

Two datasets with alpha mattes reviewed by clinicians, a subset of LIDC-IDRI [2] and the Brain-growth of QUBIQ [26], are used in this work. LIDC-IDRI dataset consists of thoracic CT scans for lung nodules diagnosis. The scans are cropped and centered into size 128×128 patches as practice [15,20]. Each patch is labeled out the region of the pulmonary nodules by four binary masks. To better focus on the uncertainty study, we select 1609 patches in which an identical nodule is labeled in the corresponding masks. The Brain-growth dataset consists of 39 low-intensity contrast T2-W MR images for the newborn brain’s white matter tissue myelination process. Each image was labeled by seven binary masks.

Alpha mattes use continuous values such that they are more capable of depicting the anatomical structures in ambiguous areas. Specifically, the uncertain region in the LIDC dataset can describe the indistinct border and ground-glass shadow around a lesion better, which is vital for nodules staging. In the Brain-growth dataset, the newborn white tissue undergoes a rapid myelination process. Thus it is hard to tag the white matter in the shifting regions myelinated or non-myelinated with a binary label.

The alpha mattes are labeled in a semi-automatic way. i.e., rough mattes are generated by matting methods and refined manually by image editors to fit the anatomical structure, which is efficient and widely used in natural image matting [29]. Here Information-Flow [1], a laplacian-based matting method, was selected to create the rough alpha mattes as its comparatively better performance in our scenario, while other methods are also possible. A trimap is required in these matting methods, which denotes the foreground, background, and unknown region as prior information. We generate it by the manual labeled masks. In particular, pixels are categorized as foreground or background only if they are tagged the same label in all the binary masks. The left inconsistent pixels are tagged as the unknown region.

Three qualified clinicians, including pediatricians and oncologists, were invited to review the various ground truth, including the proposed alpha matte and the conventional binary masks. Each of them picked the labeling to describe best the anatomical

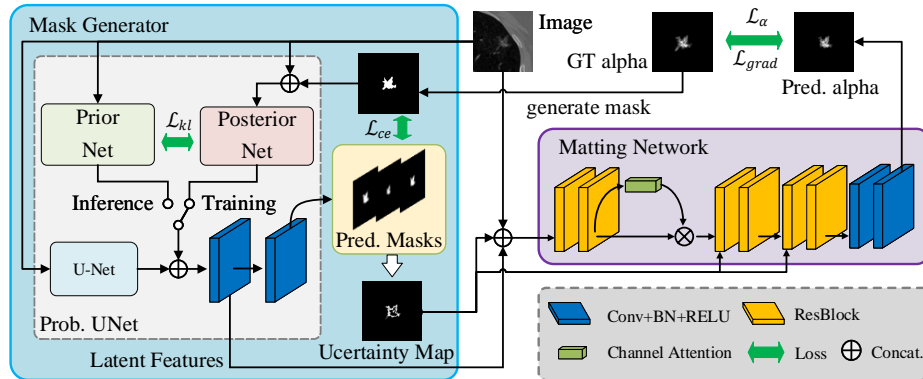


Fig. 3. The schematic diagram of Medical Matting. The Mask Generator outputs various segmentation predictions under the target distribution. Such intermediate results are merged to create an Uncertainty Map, which assists the following Matting Network like the trimap.

structures, shown in Fig. 2. It is demonstrated that the alpha mattes are significantly more favorable than the binary masks.

3 Methodology

Labeling with continuous values can accurately depict the anatomical structure and provide an intuitive way to quantify uncertainty, as shown earlier. Still, the binary mask is the mainstream segmentation method in the medical scene. Therefore, we design a multi-task network predicting the alpha matte and binary masks simultaneously to expand the application scope. Overall, the proposed medical matting framework consists of Mask Generator and Matting Network. The mask generator predicts multiple binary masks of each lesion, which can be considered a simulation of clinicians' labeling process. Then, we use the predicted score maps to build a map indicating the unsure regions, namely the uncertainty map. In the matting network, the uncertainty map, input image, and latent feature from the mask generator are merged to predict the alpha matte. Fig. 3 provides a schematic view of the framework.

3.1 Mask Generator

Mask generator can produce a bunch of binary masks, and the intermediate score maps are used to build an uncertainty map for the following matting network as assistance.

Probabilistic UNet⁴ is selected as the network to generate a set of binary masks under the target distribution. The body structures are continuous, which will also reflect in the corresponding alpha mattes. Therefore unlike the original method, which randomly

⁴ We reference to the Pytorch implementation from <https://github.com/stefanknecht/Probabilistic-Unet-Pytorch>.

samples a mask from multiple labeled masks in each training iteration, we generate a binary mask by random thresholding the ground truth alpha matte. Thus we can generate more abundant masks with structural continuity. Moreover, masks generated by different thresholds correspond to different tolerance of uncertainty. The generated mask can be formulated as Eq. 1.

$$Mask = Threshold(\alpha_{gt}, \tau), \tau \in [a, b] \quad (1)$$

where α_{gt} denotes the ground truth alpha matte, τ stands for the threshold level, a and b are practically set to 0.2 and 0.7 of the maximum of α_{gt} to get reasonable masks.

Uncertainty Map Matting methods generally introduce a priori trimap as a restriction of the foreground, background, and unknown regions, which vastly reduces the task complexity. Unlike the trimap, in medical images, it can be even difficult to tell the definite foreground, the lesions, from its surrounding structures. Inspired by the Monte Carlo dropout [18] approximation, we create a score map named uncertainty map, which indicates challenging areas to identify, playing a similar role to trimap. The uncertainty map is defined as the entropy:

$$\mathcal{U}(x) = - \sum_{c=1}^m \mathcal{P}_c(x) \log \mathcal{P}_c(x) \quad (2)$$

where $\mathcal{P}_c(x)$ is the probability of the pixel x in class c of the average score map of the probabilistic UNet predictions, and m is the number of class. Fig. 4 (d) shows examples of the generated uncertain regions.

3.2 Matting Network

The matting network outputs the alpha matte with the help of the aforementioned uncertainty map. It consists of three propagation units, and each consists of two Residual Blocks[14]. Between the first two units, a channel attention module [32] was inserted to help the network focus on effective features. The output block contains two conventional layers at the end of the pipeline. The input image, latent features from the probabilistic UNet, and the uncertainty map are concatenated as the matting network’s input. The uncertainty map is also injected at the last two propagation units as a guidance of the information flow [5].

3.3 Multi-task Loss

Multi-task learning is employed in our network for binary masks and alpha matte prediction, as it simplifies the training procedure and achieves better performance by sharing the information of the interrelated tasks. Each task is guided by its corresponding losses and balanced by an uncertainty-weighted way.

For the segmentation, following the probabilistic UNet [20] practice, Kullback-Leibler loss \mathcal{L}_{kl} and cross-entropy loss \mathcal{L}_{ce} are applied. The former is for minimizing

the divergence of the prior distribution and the posterior distribution, and the latter is for matching the generated mask and the ground truth mask.

For the matting, the absolute difference and the gradient difference between the predicted alpha matte and the ground truth alpha matte are both considered by \mathcal{L}_α and \mathcal{L}_{grad} , respectively. The gradient expresses the correlation of one pixel to its surrounding pixels, significant to the medical structure’s continuity. Moreover, a mask based on the uncertainty map is applied to make the gradient loss concentrate on the uncertain regions. The losses are defined as:

$$\mathcal{L}_\alpha(\tilde{\alpha}, \alpha_{gt}) = \frac{1}{|\tilde{\alpha}|} \sum_{i \in \alpha} \|\tilde{\alpha}(i) - \alpha_{gt}(i)\|_1 \quad (3)$$

$$\mathcal{L}_{grad}(\{\tilde{\alpha}, \mathcal{U}\}, \alpha_{gt}) = \frac{1}{|\nabla_{\tilde{\alpha}}|} \sum_{i \in \nabla_{\tilde{\alpha}}} \|\nabla_{\tilde{\alpha}}(i) - \nabla_{\alpha_{gt}}(i)\|_1, i \in \{\mathcal{U} > thresh\} \quad (4)$$

where $\tilde{\alpha}$, α_{gt} denotes the predicted and ground truth alpha matte, respectively. \mathcal{U} stands for the uncertainty map. A sub-region of \mathcal{U} selected by thresholding is used as a mask for gradient loss, which makes the loss more focused on the uncertain regions.

The outputs of each task can be assumed as each following a Gaussian distribution with observation noise. Therefore, we introduced the uncertainty weighted loss [19] to balance them. Finally, our loss \mathcal{L} is defined as:

$$\mathcal{L} = \frac{\mu \mathcal{L}_{kl} + v \mathcal{L}_{ce}}{2\sigma_1^2} + \frac{\zeta \mathcal{L}_\alpha + \xi \mathcal{L}_{grad}}{2\sigma_2^2} + \log 2\sigma_1\sigma_2 \quad (5)$$

where σ_1 and σ_2 are trainable parameters, μ , v and ζ , ξ are parameters balancing the \mathcal{L}_{kl} , \mathcal{L}_{ce} and \mathcal{L}_α , \mathcal{L}_{grad} for binary mask and alpha matte prediction, respectively.

4 Experiments

Implementation details Our method is evaluated on the datasets above with 4-fold cross-validation. The base learning rate l_r is set to 0.0001. The cosine annealing schedule [4,24] was used after a 1-epoch long steady increasing warm-up from 0 to l_r . The ADAM optimizer was used with momentum 0.9 and weight decay 5×10^{-5} . The σ_1 and σ_2 of multi-task losses are initialized to 4, and the loss weight μ is set to 10, v , ζ , ξ are set to 1. The threshold for the mask in \mathcal{L}_{grad} is set to 0.1. Sixteen masks are generated for uncertainty map generation. The LIDC-IDRI and the Brain-growth are trained 50, 100 epochs with batch-size 1, respectively. The input image is resized to 128×128 and elastic transformation [30] is deployed. All the models are trained from scratch with convolution parameters initialized by He initialization [13]. The number of generalized masks is kept the same as that of the ground truth masks during evaluation.

Results and analysis We compared the predicted alpha mattes, i.e., the calibrated uncertainty, with six state-of-the-art matting methods. The trained models of the deep-learning-based methods for the natural image are used as the data augmentation mechanism [33,11], which generate training images by randomly compose foreground and

Table 1. Quantitative comparisons with state-of-the-art matting algorithms.

Model	LIDC-IDRI				Brain-growth			
	SAD↓	MSE↓	Grad.↓	Conn.↓	SAD↓	MSE↓	Grad.↓	Conn.↓
Bayesian [8]	0.0778	0.0819	0.1535	0.0724	0.8435	0.1662	1.5921	0.8683
Closed-Form [21]	0.3040	0.4736	0.7584	0.3188	1.5419	0.4410	2.6960	1.6258
KNN [6]	0.0737	0.0451	0.1381	0.0731	0.6534	0.1073	1.1548	0.6945
Information-Flow [1]	0.0663	0.0351	0.1001	0.0652	0.6819	0.1056	1.5007	0.7209
Learning Based [36]	0.0554	0.0286	0.0826	0.0508	0.6061	0.0898	1.0559	0.6441
FBA [11]	0.0598	0.0395	0.1143	0.0557	0.7711	0.1390	1.2350	0.8220
Ours (w/o Uncertainty Map)	0.0448	0.0180	0.0414	0.0401	0.4926	0.0611	0.7692	0.5189
Ours	0.0422	0.0166	0.0401	0.0363	0.4675	0.0557	0.7123	0.4948

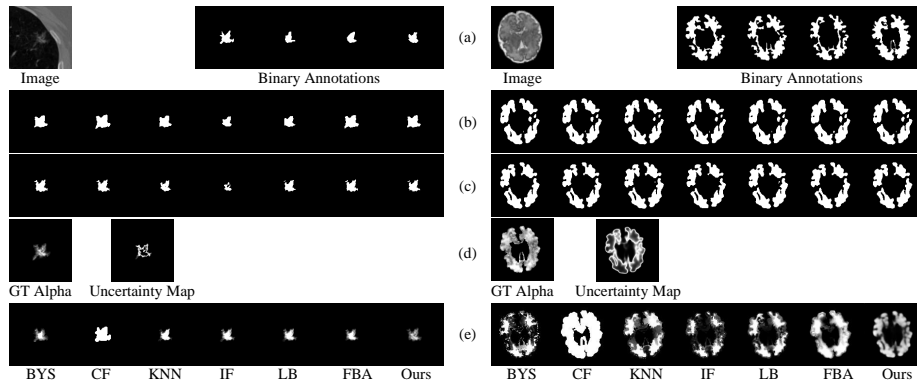


Fig. 4. Qualitative comparisons on samples from LIDC-IDRI and Brain-growth datasets. (a) original images and labeled binary masks. (b) predicted masks by Probabilistic U-net with manual binary masks. (c) predicted masks by our model with uncertainty map, which reveals more details in the ambiguity regions. (d) the target alpha mattes and the uncertainty maps in which the hard areas to recognize are highlighted. (e) the results of different matting methods. BY: Bayesian [8], CF: Closed-Form [21], KNN [6], IF: Information-Flow [1], LB: Learning Based [36], FBA [11]. Better view in zoom.

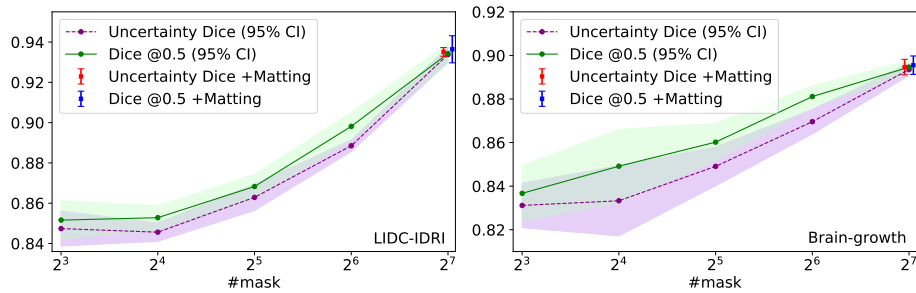


Fig. 5. The chart reveals the relationship between the number provided when training the segmentation network and the model performance. The performance grows as more masks are provided.

background, may not be anatomically correct in medical images. Moreover, we provide the methods which need a trimap with the one we used in generating the ground truth alpha mattes, mentioned in Section 2.

Tab. 1 shows that our model outperforms all the other methods in both datasets, which illustrates that our method is more applicable to the medical scenarios. It also demonstrated that the performance has a further improvement in all four metrics with the uncertainty map, indicating that the uncertainty map benefits the matting task.

The visual results are shown in Fig. 4. Our method can better express the edge of the fuzzy transition zone and subtle structural features in the matting results. Moreover, binary masks generated by our final model have a better ability to depict the details. It may be due to using the alpha matte to generate masks so that the masks also inherit the better ability of detail expression.

Ablation Study Thanks to the continuous value, alpha matte can describe the lesion structure more precisely than binary masks and quantify uncertainty intuitively. Moreover, a bunch of binary masks in the same distribution can be generated by thresholding a single alpha matte, which is advantageous over the limited manually labeled masks, reducing the labeling cost and improving efficiency. To prove it quantitatively, we investigate how the number of labeled masks used in training increase can improve the model performance. To ensure the target masks share the same distribution, we generate 128 binary masks by using Eq. 1 on alpha matte with equidistant thresholds, from which a specific number of masks is obtained by evenly sampling.

Two metrics are used to evaluate the similarity between the predicted and the ground truth masks. Uncertainty Dice $Dice_U$ is proposed to evaluate the uncertainty with multiple annotations [26] quantitatively. It can reveal the similarity of the predicted mask distribution to the target distribution by calculating the average Dice scores at different score map levels. We also adapt conventional dice with a threshold at 0.5 to the multi-label scenario, denoted as $Dice_{@0.5}$, to reveal the similarity to a specific target mask instead of overall performance. The metrics are formulated as:

$$Dice_U(\tilde{\mathcal{P}}, \mathcal{D}_{gt}) = \frac{1}{|\mathcal{T}|} \sum_{\tau \in \mathcal{T}} \frac{1}{|\tilde{\mathcal{P}}|} \sum_{\tilde{p} \in \tilde{\mathcal{P}}} Dice(Threshold(\tilde{p}, \tau), \mathcal{D}_{gt}) \quad (6)$$

$$Dice_{@0.5}(\tilde{\mathcal{M}}, \mathcal{M}_{gt}) = \frac{1}{|\tilde{\mathcal{M}}|} \sum_{\tilde{m} \in \tilde{\mathcal{M}}} max\{Dice(\tilde{m}, m_{gt}), m_{gt} \in \mathcal{M}_{gt}\} \quad (7)$$

where $\tilde{\mathcal{P}}$ is the set of predicted score maps. \mathcal{D}_{gt} denotes the ground truth distribution, calculated by averaging the target masks. \mathcal{T} is a set of thresholds, that $\mathcal{T} = \{\tau | 0.05, 0.15, \dots, 0.95\}$. $\tilde{\mathcal{M}}$ and \mathcal{M}_{gt} denote the predicted and target masks, respectively.

We deployed experiments on probabilistic UNet with different numbers of masks, ranging from 8 to 128. Fig. 5 shows the results. It is demonstrated that both metrics' results grow as more masks are provided. It also reveals that alpha matte is a promising annotation form in medical segmentation that can achieve comparable performance with much more binary labels. Moreover, an additional experiment was deployed to compare the performance of the Probabilistic UNet and our model. We find the performance can be improved with our model, which indicates training with the matting

network may improve the performance, and the matting task benefits the binary segmentation task (Fig. 5 +Matting).

5 Conclusions

In this work, we creatively calibrate the uncertainty by alpha matte introduced from image matting, which has a better ability to reveal tiny and ambiguous structures and has a big potential for diagnosis. A well-designed multi-task network was proposed to predict binary masks and alpha matte simultaneously. The uncertainty map, an analogy to trimap, is generated by the intermediate outputs and improves the matting network performance. The binary masks, uncertainty map, and alpha matte express the target with uncertainty in different aspects, so the sub-tasks can benefit each other by sharing the latent information during training. Experiments reveal our model outperforms the other state-of-the-art matting methods on all four metrics with a considerable margin and demonstrate that alpha matte is a more powerful annotation method than the binary mask. We labeled two datasets with alpha matte, including CT and MRI images, and they are released to the public to promote the study on uncertainty learning and matting in medical scenarios. More modalities will be examined with medical matting, and also new experiments will be carried out to test its value in diagnosis in the future.

Acknowledgements The authors would like to thank the clinicians for their hard work in evaluating the alpha matte datasets. They are Yi Luo of Chongqing hospital of traditional Chinese medicine, Huan Luo of Chongqing Renji Hospital of Chinese Academy of Sciences, and Feng Jiang of the First Affiliated Hospital of Wenzhou Medical University.

References

1. Aksoy, Y., Ozan Aydin, T., Pollefeys, M.: Designing effective inter-pixel information flow for natural image matting. In: Proceedings of the IEEE Conference on Computer Vision and Pattern Recognition (CVPR). pp. 29–37 (2017)
2. Armato III, S.G., McLennan, G., McNitt-Gray, M.F., Meyer, C.R., Yankelevitz, D., Aberle, D.R., Henschke, C.I., Hoffman, E.A., Kazerooni, E.A., MacMahon, H., et al.: Lung image database consortium: developing a resource for the medical imaging research community. *Radiology* **232**(3), 739–748 (2004)
3. Baumgartner, C.F., Tezcan, K.C., Chaitanya, K., Hötter, A.M., Muehlematter, U.J., Schawkat, K., Becker, A.S., Donati, O., Konukoglu, E.: Phiseg: Capturing uncertainty in medical image segmentation. In: International Conference on Medical Image Computing and Computer-Assisted Intervention (MICCAI). pp. 119–127. Springer (2019)
4. Bochkovskiy, A., Wang, C.Y., Liao, H.Y.M.: Yolov4: Optimal speed and accuracy of object detection. arXiv preprint arXiv:2004.10934 (2020)
5. Cai, S., Zhang, X., Fan, H., Huang, H., Liu, J., Liu, J., Liu, J., Wang, J., Sun, J.: Disentangled image matting. In: Proceedings of the IEEE International Conference on Computer Vision (ICCV). pp. 8819–8828 (2019)
6. Chen, Q., Li, D., Tang, C.K.: KNN Matting. *IEEE Transactions on Pattern Analysis and Machine Intelligence (TPAMI)* **35**(9), 2175–2188 (2013)

7. Cheng, J., Zhao, M., Lin, M., Chiu, B.: Awm: Adaptive weight matting for medical image segmentation. In: *Medical Imaging 2017: Image Processing*. vol. 10133, p. 101332P. International Society for Optics and Photonics (2017)
8. Chuang, Y.Y., Curless, B., Salesin, D.H., Szeliski, R.: A bayesian approach to digital matting. In: *Proceedings of the IEEE Conference on Computer Vision and Pattern Recognition (CVPR)*. vol. 2, pp. II–II. IEEE (2001)
9. Der Kiureghian, A., Ditlevsen, O.: Aleatory or epistemic? does it matter? *Structural safety* **31**(2), 105–112 (2009)
10. Fan, Z., Lu, J., Wei, C., Huang, H., Cai, X., Chen, X.: A hierarchical image matting model for blood vessel segmentation in fundus images. *IEEE Transactions on Image Processing (TIP)* **28**(5), 2367–2377 (2018)
11. Forte, M., Pitić, F.: F, B, Alpha Matting. arXiv preprint arXiv:2003.07711 (2020)
12. Gantenbein, M., Erdil, E., Konukoglu, E.: Revphiseg: A memory-efficient neural network for uncertainty quantification in medical image segmentation. In: *Uncertainty for Safe Utilization of Machine Learning in Medical Imaging, and Graphs in Biomedical Image Analysis*, pp. 13–22. Springer (2020)
13. He, K., Zhang, X., Ren, S., Sun, J.: Delving deep into rectifiers: Surpassing human-level performance on imagenet classification. In: *Proceedings of the IEEE International Conference on Computer Vision (CVPR)*. pp. 1026–1034 (2015)
14. He, K., Zhang, X., Ren, S., Sun, J.: Deep residual learning for image recognition. In: *Proceedings of the IEEE conference on computer vision and pattern recognition (CVPR)*. pp. 770–778 (2016)
15. Hu, S., Worrall, D., Knekt, S., Veeling, B., Huisman, H., Welling, M.: Supervised uncertainty quantification for segmentation with multiple annotations. In: *International Conference on Medical Image Computing and Computer-Assisted Intervention (MICCAI)*. pp. 137–145. Springer (2019)
16. Hüllermeier, E., Waegeman, W.: Aleatoric and epistemic uncertainty in machine learning: A tutorial introduction. arXiv preprint arXiv:1910.09457 (2019)
17. Kendall, A., Badrinarayanan, V., Cipolla, R.: Bayesian segnet: Model uncertainty in deep convolutional encoder-decoder architectures for scene understanding. In: *British Machine Vision Conference (BMVC)* (2017)
18. Kendall, A., Gal, Y.: What uncertainties do we need in bayesian deep learning for computer vision? In: *Advances in Neural Information Processing Systems (NIPS)*. pp. 5574–5584 (2017)
19. Kendall, A., Gal, Y., Cipolla, R.: Multi-task learning using uncertainty to weigh losses for scene geometry and semantics. In: *Proceedings of the IEEE Conference on Computer Vision and Pattern Recognition (CVPR)*. pp. 7482–7491 (2018)
20. Kohl, S., Romera-Paredes, B., Meyer, C., De Fauw, J., Ledsam, J.R., Maier-Hein, K., Eslami, S.A., Rezende, D.J., Ronneberger, O.: A probabilistic U-Net for segmentation of ambiguous images. In: *Advances in Neural Information Processing Systems (NIPS)*. pp. 6965–6975 (2018)
21. Levin, A., Lischinski, D., Weiss, Y.: A closed-form solution to natural image matting. *IEEE Transactions on Pattern Analysis and Machine Intelligence (TPAMI)* **30**(2), 228–242 (2007)
22. Li, Y., Lu, H.: Natural image matting via guided contextual attention. In: *Proceedings of the AAAI Conference on Artificial Intelligence (AAAI)*. vol. 34, pp. 11450–11457 (2020)
23. Li, Y., Xu, Q., Lu, H.: Hierarchical opacity propagation for image matting. arXiv preprint arXiv:2004.03249 (2020)
24. Loshchilov, I., Hutter, F.: SGDR: Stochastic gradient descent with warm restarts. *Learning* **10**, 3
25. Lutz, S., Amplianitis, K., Smolic, A.: Alphagan: Generative adversarial networks for natural image matting. arXiv preprint arXiv:1807.10088 (2018)

26. Menze, B., Joskowicz, L., Bakas, S., Jakab, A., Konukoglu, E., Becker, A.: Quantification of uncertainties in biomedical image quantification challenge. [EB/OL], <https://qubiq.grand-challenge.org/Home/> Accessed October 22, 2020
27. Monteiro, M., Folgoc, L.L., de Castro, D.C., Pawlowski, N., Marques, B., Kamnitsas, K., van der Wilk, M., Glocker, B.: Stochastic segmentation networks: Modelling spatially correlated aleatoric uncertainty. arXiv preprint arXiv:2006.06015 (2020)
28. Rupprecht, C., Laina, I., DiPietro, R., Baust, M., Tombari, F., Navab, N., Hager, G.D.: Learning in an uncertain world: Representing ambiguity through multiple hypotheses. In: Proceedings of the IEEE International Conference on Computer Vision (ICCV). pp. 3591–3600 (2017)
29. Shen, X., Tao, X., Gao, H., Zhou, C., Jia, J.: Deep automatic portrait matting. In: European Conference on Computer Vision (ECCV (2016)
30. Simard, P.Y., Steinkraus, D., Platt, J.C., et al.: Best practices for convolutional neural networks applied to visual document analysis. In: Icdar. vol. 3 (2003)
31. Wang, G., Li, W., Aertsen, M., Deprest, J., Ourselin, S., Vercauteren, T.: Aleatoric uncertainty estimation with test-time augmentation for medical image segmentation with convolutional neural networks. *Neurocomputing* **338**, 34–45 (2019)
32. Woo, S., Park, J., Lee, J.Y., So Kweon, I.: CBAM: Convolutional block attention module. In: Proceedings of the European Conference on Computer Vision (ECCV). pp. 3–19 (2018)
33. Xu, N., Price, B., Cohen, S., Huang, T.: Deep image matting. In: Proceedings of the IEEE Conference on Computer Vision and Pattern Recognition (CVPR). pp. 2970–2979 (2017)
34. Zeng, Z., Wang, J., Shepherd, T., Zwiggelaar, R.: Region-based active surface modelling and alpha matting for unsupervised tumour segmentation in pet. In: IEEE International Conference on Image Processing (ICIP). pp. 1997–2000. IEEE (2012)
35. Zhao, H., Li, H., Cheng, L.: Improving retinal vessel segmentation with joint local loss by matting. *Pattern Recognition (PR)* **98**, 107068 (2020)
36. Zheng, Y., Kambhamettu, C.: Learning based digital matting. In: 2009 IEEE 12th international conference on computer vision (ICCV). pp. 889–896. IEEE (2009)